Supporting Information

Generation of hot electrons with chiral metamaterial perfect absorbers: giant optical chirality for polarization-sensitive photochemistry

Wenhao Wang,[†] Lucas V. Besteiro,[†,‡] Tianji Liu,[†,§] Cuo Wu,[†] Jiachen Sun,[†] Peng Yu,[†] Le Chang,[†] Zhiming Wang,[*,†] and Alexander O. Govorov,[*,†,∥]

[†]*Institute of Fundamental and Frontier Sciences, University of Electronic Science and Technology of China, Chengdu 610054, China*

[‡]*Centre Énergie Matériaux et Télécommunications, Institut National de la Recherche Scientifique, Varennes, Quebec J3X 1S2, Canada*

[§]*Graduate School of Engineering, Osaka University, 2-1 Yamadaoka, Suita, Osaka 565-0871, Japan*

[∥]*Department of Physics and Astronomy, Ohio University, Athens, Ohio 45701, United States*

**E-mail: zhmwang@uestc.edu.cn and govorov@ohio.edu*

6 pages, 7 figures, 1 table.

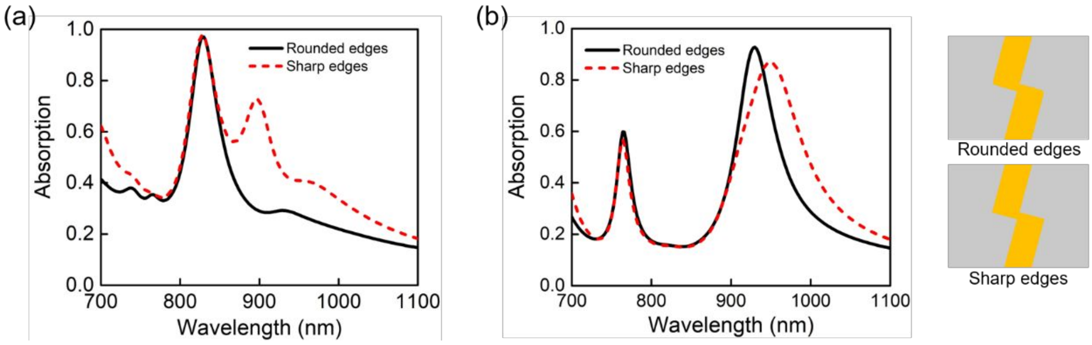

Figure S1. Simulated optical absorption spectra of LH metamaterials with rounded (black solid line) and sharp (red dashed line) edges, under the incidence of (a) LCP and (b) RCP light. The insets in the right show the top view of metamaterials with and without rounded corners, respectively. The rounded edges have a radius of curvature of 10 nm. These data make clear how relevant is to carefully consider the modelling of sharp features in plasmonic nanostructures, because introducing the, physically unrealistic, perfectly sharp corners produce additional plasmonic resonances that will not be present in a realistic system.

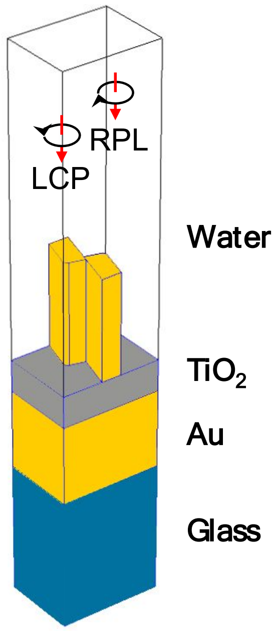

Figure S2. 3D view of the model used in the simulation of the metamaterial. The LCP and RCP light is perpendicularly incident on its surface, propagating from the top boundary. The incident energy flux is set as $I_0 = 10^5$ W/cm^2. Periodic boundary conditions are applied on the vertical walls of the simulation cell, simulating an infinite 2D metamaterial decorated with parallel wire-shaped antenna arrays. A very fine mesh, with a minimum element size of 0.4 nm, was used to discretize the antenna and precisely calculate the strong electromagnetic enhancement occurring at its edges. Perfectly matched layers are used at the top of the water domain and at the bottom of the glass domain, simulating the behavior of infinite dielectric domains in the vertical direction.

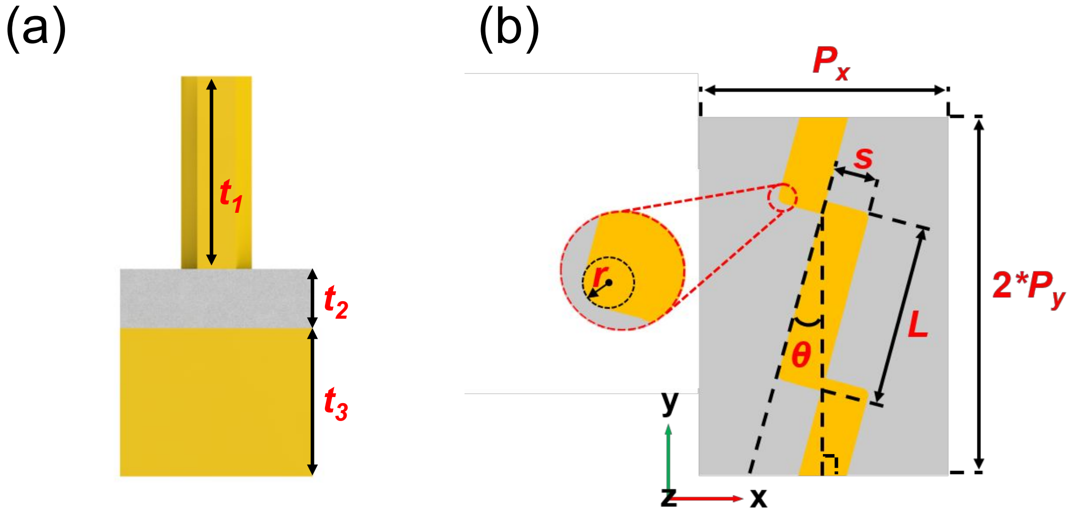

Figure S3. (a) Side view and (b) top view of the replicated geometry that conforms the metamaterial, twice the size of its unit cell. The key geometric parameters are shown in Table S1.

Table S1. Parameters of the metamaterial geometry

Thickness of the top Au nanoantenna, t_1 (nm)	260
Thickness of the TiO_2 layer, t_2 (nm)	80
Thickness of the bottom Au film, t_3 (nm)	200
Radius of the rounded corner of Au cuboid, r (nm)	10
Length of Au cuboid, L (nm)	200
Width of Au cuboid, s (nm)	50
Rotation angle of Au cuboid, θ (°)	15
Period in the x-axis direction, P_x (nm)	260
Period in the y-axis direction, $P_y=s/\sin(\theta)$ (nm)	193

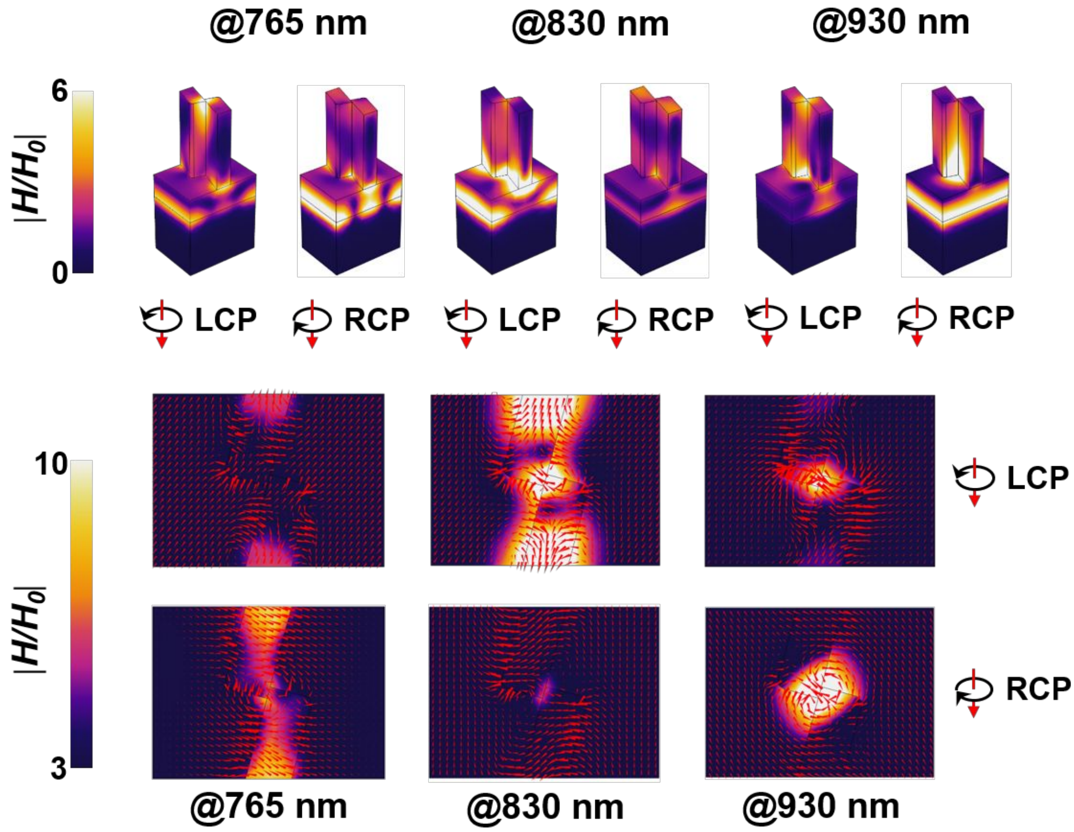

Figure S4. Simulated magnetic fields on the walls of the metamaterial and at the interface between metal wire antenna and dielectric spacer. The data is presented for both LCP and RCP illumination, at the wavelengths of 765 nm, 830 nm, and 930 nm. The red arrow in the planar magnetic fields indicates the displacement current.

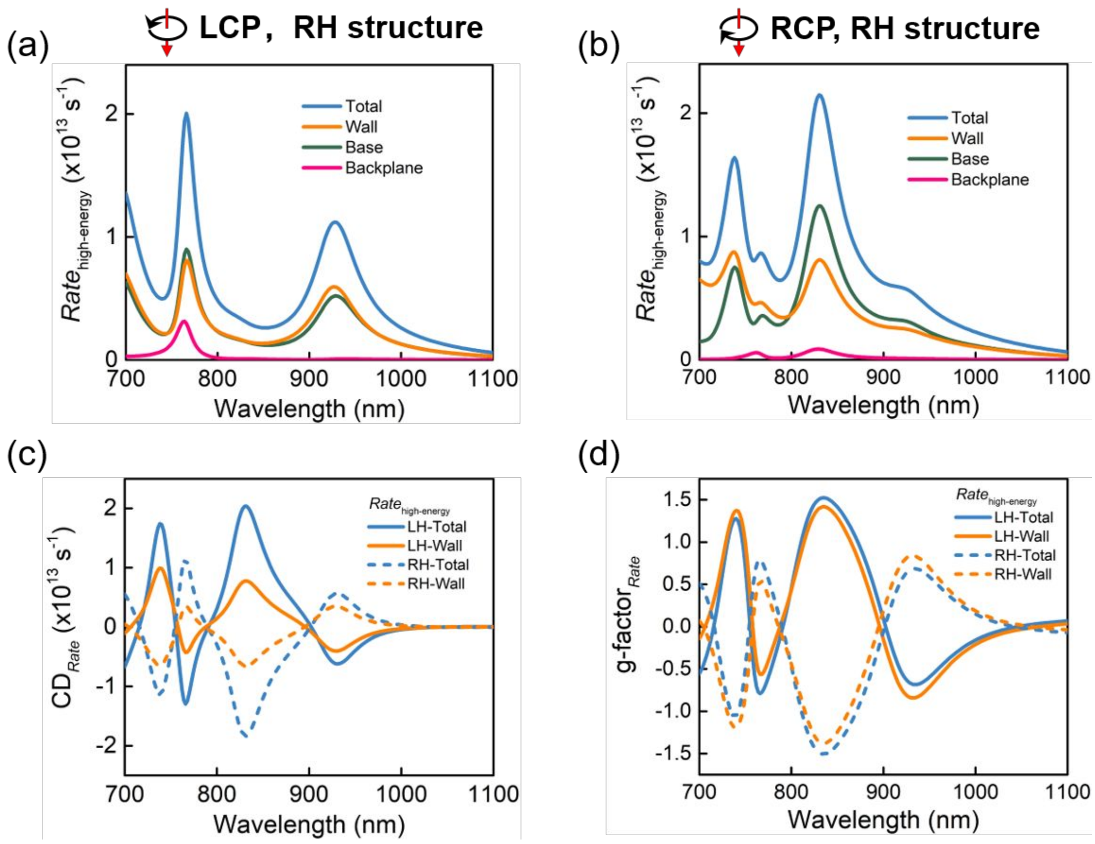

Figure S5. The simulated $Rate_{\text{high energy}}$ results for the outer walls (yellow), the nanoantenna's base (green), the backpanel (pink) and the total surface area (blue) of the RH metamaterial under the illumination of (a) LCP and (b) RCP light. (c) CD and (d) g-factor spectrum of $Rate_{\text{high energy}}$ (blue) and $Rate_{\text{high energy, wall}}$ (yellow) of the LH (solid line) and the RH (dotted line) enantiomers. The LH and RH metamaterials possess opposite CD and g-factor curve, with a maximum of 2.04 x 10^{13} s^{-1} and 1.52, respectively.

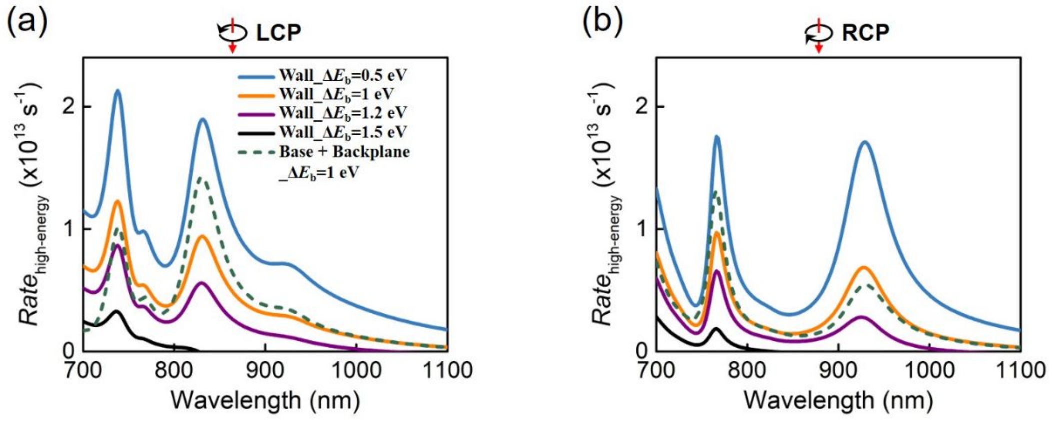

Figure S6. The effect of the height of potential barrier formed between Au-TiO_2 and Au-water interface on the $Rate_{\text{high energy}}$. Simulated $Rate_{\text{high energy}}$ results for different interface of the LH metamaterial under the illumination of (a) LCP and (b) RCP light. Different potential barrier formed between Au-water, ΔE_b = 0.5 eV (blue), 1 eV (yellow), 1.2 eV (purple) and 1.5 eV (black), are chosen to calculate the $Rate_{\text{high energy}}$ for the outer walls, so as to represent a range of injection conditions into molecular adsorbates. The potential barrier formed between Au-TiO_2 is fixed at 1 eV to calculate $Rate_{\text{high energy}}$ for the nanoantenna's base and the backplane, which are summed together (green dashed line) to provide a baseline for comparison to the injection through the outer walls. With different potential barrier heights, ΔE_b, calculated $Rate_{\text{high energy}}$ at the walls preserve their overall shape, which means the polarization dependent effect of $Rate_{\text{HE}}$ is robust for different potential barrier. Two main changes occur when modifying the barrier's height: (1) For reactions with a lower barrier, the wall-injected hot electrons will dominate the behavior of the system, and it is a situation that would be representative of several experimental contexts. (2) The disappearance of the low-energy peaks of $Rate_{\text{high energy, wall}}$, near 830 nm for LCP light and 930 nm for RCP light, when ΔE_b = 1.5 eV (black curves). This is due to the incident energy carried at these longer wavelengths being insufficient to create over-barrier excited electrons. The cut-off wavelength (λ_{cutoff}) for this barrier height is 827 nm.

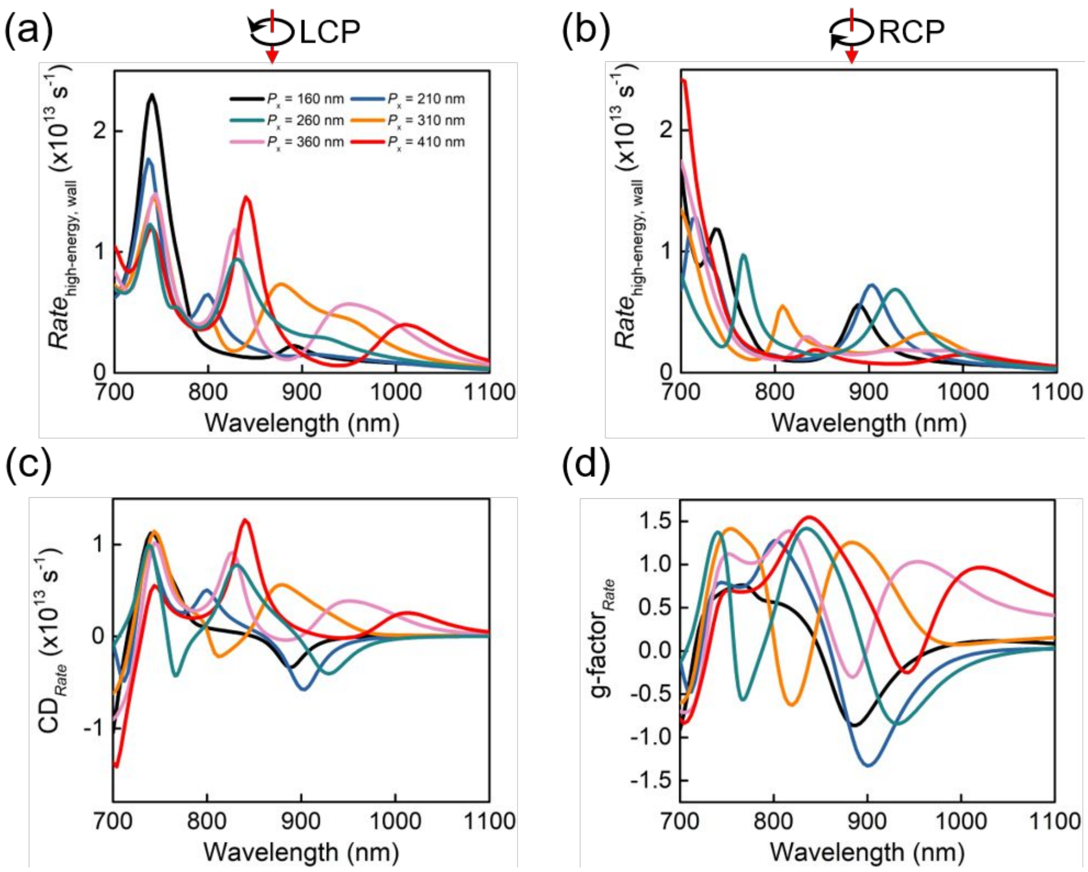

Figure S7. $Rate_{\text{high-energy, wall}}$ spectrum of a LH metamaterial as a function of P_x for (a) LCP and (b) RCP illumination. (c) CD and (d) g-factor of $Rate_{\text{high-energy, wall}}$ of a LH metamaterial as a function of P_x. P_x = 160 (black), 210 (blue), 260 (green), 310 (yellow), 360 (pink), and 410 nm (red).